ORNL/TM-2024/ 3611

New ASME Section III, Division 5 Creep-Fatigue Design Rules Based on EPP and SMT Approaches

Yanli Wang

October 2024

Approved for public release.
Distribution is unlimited.

OAK RIDGE National Laboratory

ORNL IS MANAGED BY UT-BATTELLE LLC FOR THE US DEPARTMENT OF ENERGY

ORNL/TM-2024/ 3611

Materials Science and Technology Division

NEW ASME SECTION III, DIVISION 5 CREEP-FATIGUE DESIGN RULES BASED ON EPP AND SMT APPROACHES

Yanli Wang

Date Published: October 2024

Prepared by
OAK RIDGE NATIONAL LABORATORY
Oak Ridge, TN 37831
managed by
UT-BATTELLE LLC
for the
US DEPARTMENT OF ENERGY
under contract DE-AC05-00OR22725

Page intentionally left blank.

CONTENTS

LIST OF FIGURES

LIST OF TABLES

ABBREVIATIONS

ANL	Argonne National Laboratory
ART	Advanced Reactor Technologies
ASME	American Society of Mechanical Engineers
BPVC	Boiler and Pressure Vessel Code
CF	creep-fatigue
DOE	US Department of Energy
EPP	elastic-perfectly plastic
GCR	Gas-Cooled Reactors
INL	Idaho National Laboratory
NE	Office of Nuclear Energy
ORNL	Oak Ridge National Laboratory
pSMT	internal-pressurized simplified model test
SB-pSMT	single-bar internal-pressurized simplified model test
SBSMT	single-bar simplified model test
SMT	simplified model test
US-NRC	U.S. Nuclear Regulatory Commission

ACKNOWLEDGMENTS

This research was sponsored by the US Department of Energy (DOE) under contract no. DE-AC05-00OR22725 with Oak Ridge National Laboratory (ORNL), managed and operated by UT-Battelle LLC. Programmatic direction was provided by the Office of Nuclear Reactor Deployment of the DOE Office of Nuclear Energy (NE).

The author would like to express her gratitude to Sue Lesica, Federal Materials Lead for the DOE-NE Advanced Reactor Technologies (ART) Program; Matthew Hahn, Federal Program Manager of the ART Gas-Cooled Reactors (GCR) Campaign; and Gerhard Strydom of Idaho National Laboratory (INL), National Technical Director of the ART GCR Campaign, for their invaluable support.

The author would like to thank Bradley J. Hall of ORNL for his technical support in conducting the experiments. Additionally, the author acknowledges Peijun Hou of Imtech Incorporation, Knoxville, TN, for analyzing previous experimental data; subject matter expert Robert I. Jetter for his valuable technical input; and Mark Messner of Argonne National Laboratory for his modeling support and insights.

Special thanks are extended to Ting-Leung Sham of the U.S. Nuclear Regulatory Commission (US-NRC), who served as the Advanced Materials Technology Area Lead for the ART Program within DOE-NE and supported this work prior to joining the US-NRC in FY 2024.

The time spent by Lianshan Lin and Xuesong Fan of ORNL reviewing this report is acknowledged.

ABSTRACT

The integrated elastic-perfectly plastic (EPP) and simplified model test (SMT) creep-fatigue (CF) design methodology, referred to as the EPP-SMT method, is being developed as an alternative for CF evaluation in the design of pressure boundary components for high-temperature reactors. This report reviews the conceptual basis of the EPP-SMT methodology, summarizes the SMT experimental development efforts and results, and provides the technical basis for finalizing the EPP-SMT CF design curves for Alloy 617, based on a combined experimental and numerical approach conducted in FY 2024.

This report presents the effect of hold time on the CF design curves for Alloy 617 at elevated temperatures. It includes proposed EPP-SMT CF design curves and tabulated values for continuous cycling, along with the effects of maximum hold time, for the use of this EPP-SMT CF evaluation method.

1. BACKGROUND

Creep-fatigue (CF) interaction damage is the primary damage mode for high-temperature structural components subjected to cyclic loading. Over the past several decades, researchers within the American Society of Mechanical Engineers (ASME) Boiler and Pressure Vessel Code (BPVC), Section III, Division 5, have focused on developing elevated temperature code rules to ensure conservative structural designs that mitigate CF failure in high-temperature reactors. Generally, advancements in the CF evaluation of structural materials are crucial for improving the economic viability of high-temperature reactors. The current evaluation procedure for CF damage in Subsection HB, Subpart B of BPVC Section III, Division 5 relies on the bilinear CF integration damage diagram, known as the D-diagram approach. However, this analysis method is complex and often leads to excessively conservative designs, which arises from how the D-diagram was constructed from the standard CF data, along with the conservative procedures used in the CF design analysis.

The integrated elastic-perfectly plastic (EPP) and simplified model test (SMT) design methodology, referred to as the EPP-SMT method, is being developed as an alternative approach for evaluating CF in the design of pressure boundary components for high-temperature reactors. The key in this new alternative CF evaluation approach is that it no longer requires the use of the damage interaction diagram, and the combined effects of creep and fatigue are accounted for in the SMT testing data. In developing this method, the SMT specimens are designed to replicate or bound the stress and strain redistribution that occurs in actual components when loaded in the creep regime, effectively account for increased creep damage around localized defects and stress risers. On the other hand, the EPP methods greatly simplify the design evaluation procedure by eliminating the need for stress classification, which is the basis of the current simplified design rules. This method aims to combine the advantages of both EPP and SMT CF evaluation techniques while reducing the over-conservatism found in the current D-diagram CF evaluation procedures.

This report summarizes the key steps in developing the EPP-SMT methodology. It also includes a summary of the SMT-based experimental results for Alloy 617. The EPP-SMT design curves for Alloy 617 are developed by integrating experimental data with extrapolation from a material model.

2. TECHNICAL BASIS OF EPP-SMT METHOD

2.1 CONCEPTUAL BASIS OF THE EPP-SMT APPROACH

2.1.1 Elastic follow-up effect

Materials subjected to cyclic deformation at elevated temperatures experience both creep and fatigue damage. These two mechanisms can interact, significantly impacting the overall performance and durability of the material. CF interaction damage under cyclic loading at elevated temperatures is often more detrimental than either pure fatigue or pure creep damage alone.

In high-temperature structural components, creep deformation can lead to stress and strain redistribution at stress riser locations, including both structural and metallurgical discontinuities. This phenomenon is known as the "elastic follow-up" effect. Elastic follow-up can result in larger accumulated strains in structures subjected to displacement-controlled loading than those predicted by elastic analysis. This effect accelerates damage to the material and may cause failure in components under long-term loading. Understanding this effect and developing design approaches to account for it are crucial for predicting the performance and lifespan of structural components under complex loading conditions.

Referring to Figure 1, elastic follow-up can be quantified by calculating the ratio of the creep strain in the test section of a component—including the effects of elastic follow-up, ε_{0-2}, —to the creep strain that would have occurred under pure relaxation, ε_{0-1}. The latter represents the condition where standard strain-controlled CF is conducted on a laboratory-scale test coupon specimen.

Thus, the elastic follow-up factor, q, is given by:

$$q = (\varepsilon_{0-2})/(\varepsilon_{0-1})$$

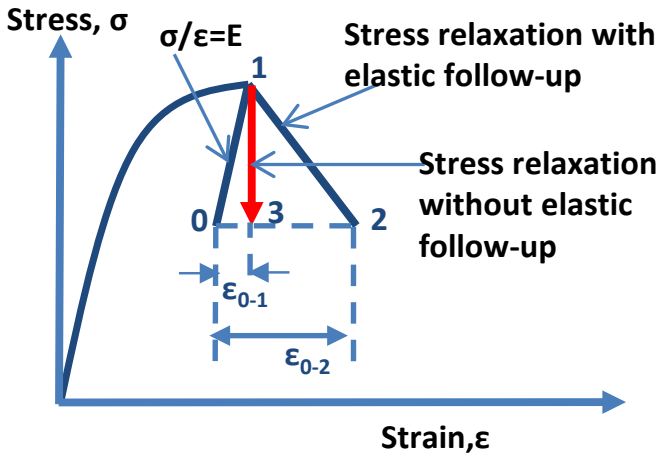

Figure 1. Elastic follow-up.

More recently, Messner et al. (2019) described a method for determining the elastic follow-up factor in 3D finite element calculations as a function of position and time from finite element simulations. They demonstrated that classical elastic-creep solutions can be utilized to assess elastic follow-up and to develop representative values for high-temperature components.

2.1.2 EPP-SMT creep-fatigue evaluation approach

The basic concept of the EPP-SMT CF evaluation methodology is shown in Figure 2. The high temperature structural component design features a stepped cylinder with a stress concentration at the shoulder fillet radius, similar to that found in tube-sheet heat exchanger structures. The component has a global elastic follow-up, q_n, which is due to the interaction between the two cylindrical sections, and a local follow-up, q_p, which is due to the local stress concentration. If the thick cylinder is displaced radially inward a fixed amount, δ_{comp}, there will be a maximum strain at the area where stress concentration occurs. Damage to the structure from a strain, $\varepsilon_{E,comp}$, that is applied, held, and then cycled back to zero and reapplied accumulates over its life span.

In high temperature SMT CF experiments, the tests are designed to simulate the key features of high-temperature components, including the elastic follow-up factor, q_{test}, stress concentration, K, and conditions with primary pressure load. The effects of plasticity, creep and strain redistribution are accounted for in the SMT CF key feature testing simulation.

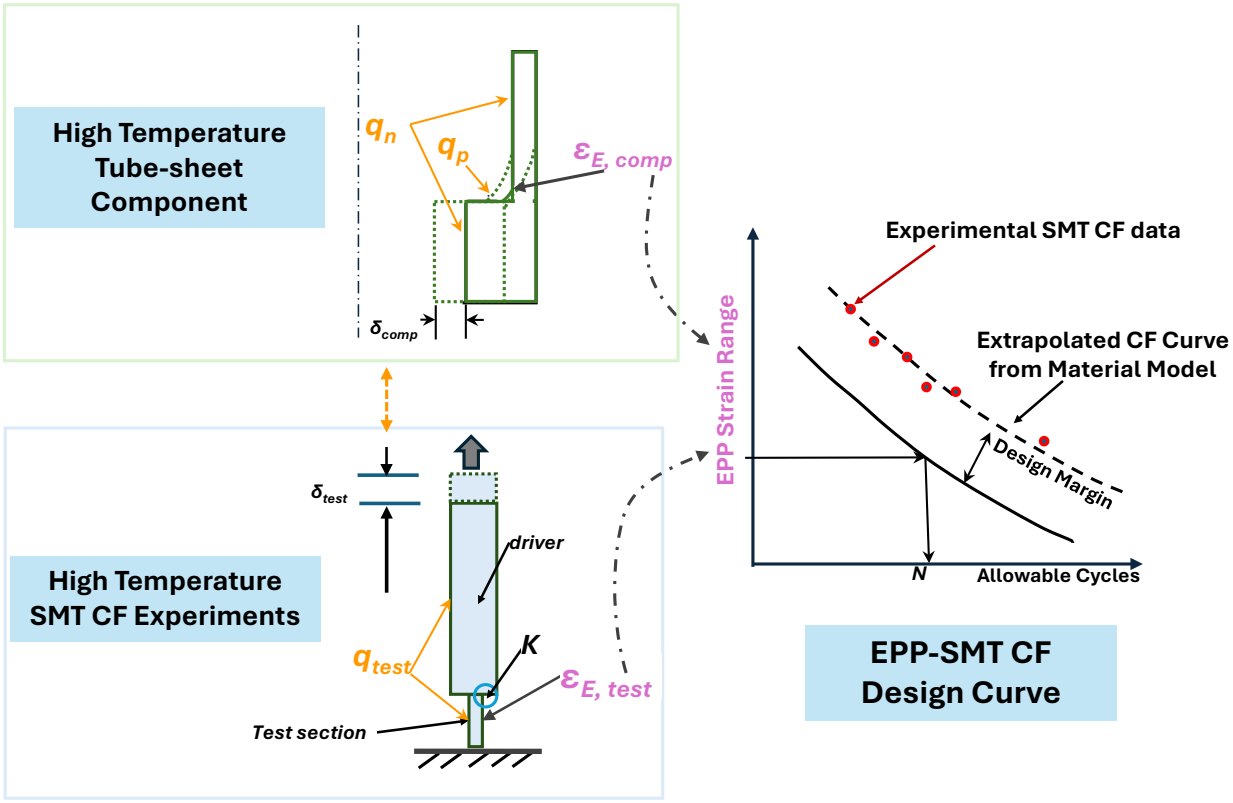

Figure 2. Conceptual overview of the EPP-SMT methodology.

The key relevant parameters in this approach are the calculated maximum strain in the structural component and the strain range in the SMT test article. In the EPP-SMT methodology, the maximum strain ranges for both the high temperature component and the SMT test specimens are determined using the EPP strain limits procedure outlined in Code Case N-861.

In practice, generating the experimental SMT CF data required to establish the design curve is often impractical, particularly at low strain ranges and extended hold times. In this study, a well-calibrated material constitutive model developed at ANL was used to generate the information needed for developing the EPP-SMT CF design curves.

The evaluation procedure using this EPP-SMT approach is essentially the same as that used in Subsection NB, where the damage fraction is determined as the ratio of actual number of cycles to the allowed number of cycles. The CF design curve includes the effects of hold time duration and the necessary adjustments to account for the elastic follow-up effect without being excessively conservative.

2.2 SMT CHARACTERISTICS AND EXPERIMENTS

SMT experiments utilize a two-bar geometry to bound the response of a high-temperature component. While there is no rigorous method to conclusively demonstrate that this two-bar model can bound the deformation of a structural component under all conditions, approaches based on a four-bar model representation of the stepped cylinder can be employed to show that the bounding strategy is applicable across a variety of practical scenarios (Kasahara et al. 1995; Jetter 1998).

There are two types of geometric limitations. The first is the allowable value of local stress concentration when combined with the effects of global elastic follow-up. In high-temperature components, it is crucial to avoid structural designs where the stresses at local stress concentrations do not relax. A high stress concentration in areas with structural or metallurgical discontinuities and significant global elastic follow-up can lead to a nonlinear increase in localized strain range, resulting in accelerated creep damage, and premature failure.

By requiring that the stress at the local stress concentration relax and using an expression for the relaxation rate developed by Kasahara et al. (1995), Jetter (1998) established a restriction on elastic stress concentration, K, as a function of global follow-up q_n as $K \leq \frac{q_n}{q_n - 1}$. He also provided an expression for the peak combined follow-up, q_p, in the four-bar structure for a range of practical values of K and q_n as $q_p \leq Kq_n$. This expression for peak elastic follow-up was also recommended by Takahura et al. 1995, based on thermal transient testing of a cylindrical shell using a notch model and a stepped cylinder model. Jetter (1998) noted that the value of global follow-up is conservatively represented by $q_n = 2$, and is certainly bounded by a value of 3, provided the stress range and stress concentration are appropriately limited for the high-temperature components. Consequently, the global elastic follow-up for representative structures suggests that the follow-up for an SMT specimen should fall within the range of 4.0 to 4.5 to adequately bound the response of the structures of interest.

However, recent analysis by Messner et al. (2019), using a full inelastic analysis of flat-head components, showed that in highly localized areas at stress concentration locations, the local elastic follow-up can be as high as q=12. Therefore, it is recommended to adjust the EPP-SMT CF design analysis according to the elastic follow-up factor relevant to the specific design problems being examined.

A detailed plan was developed and subsequently revised for the development of this EPP-SMT methodology (Wang et al. 2016a, 2016b, 2017a, 2018, 2019; Messner 2018). SMT-based design methodology is an experimental data-based approach. The development of SMT-based design curves requires experimental data, and the parameters to be considered include elastic follow-up factor, strain range, strain rate, testing temperature, hold time, and primary load. The challenges in laboratory-scale SMT experiments are the geometric limitations to achieve the magnitude of global follow-up, q_n, in the representative structure to bound the response of representative structures of interest.

Photographs of the regenerative SMT experimental articles used in this program are shown in Figure 3, and the SMT experimental design is summarized in Table 1. SMT data were generated using both key feature SMT articles and standard lab-scale specimens for comparative analysis. In the original SMT key feature testing methods, the elastic follow-up factor was established by adjusting the length and area ratios of the driver section to the test section (Wang et al. 2013, 2014, 2015, 2016a, 2017b, 2017c). The original SMT key feature testing includes two types of stepped solid round bar test articles and stepped tubular test articles designed for testing under internal pressure, pSMT. To effectively represent creep damage characteristics through key feature SMT, especially at very high temperatures, the specimen configurations often become costly and may exceed the limits of test control and stability.

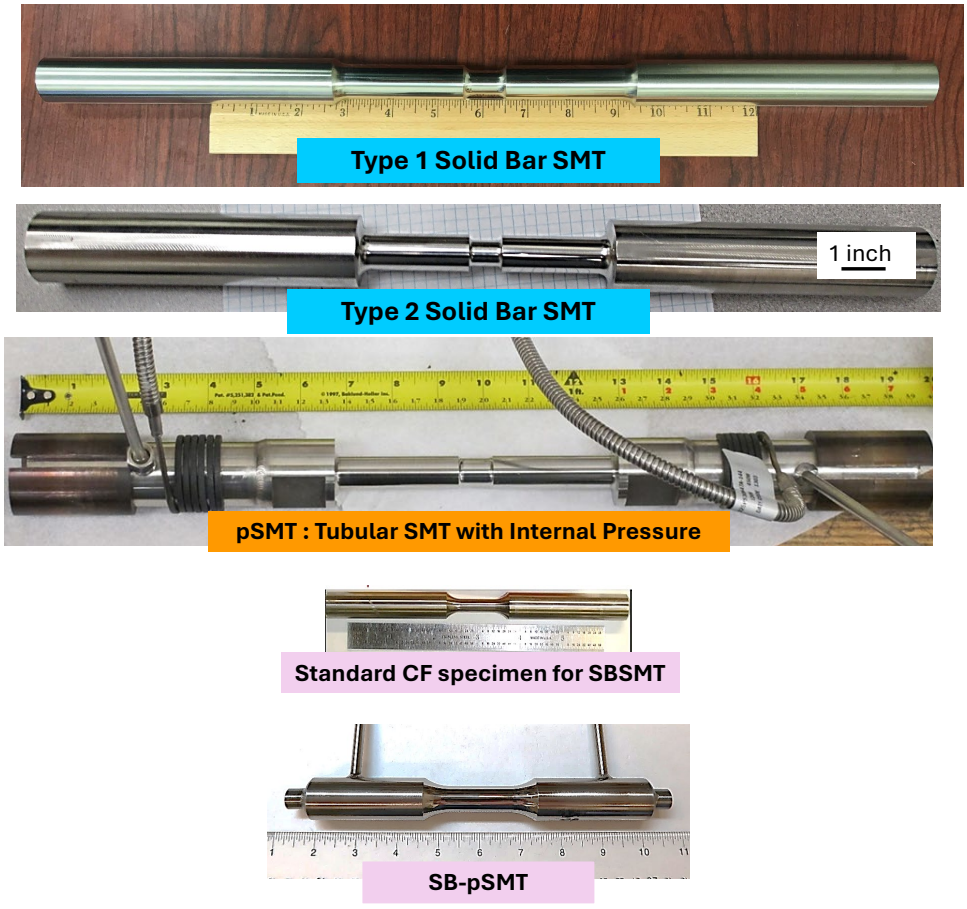

Figure 3. SMT test articles for Alloy 617.

Table 1. Design of the SMT experiments.

SMT experiment design	Elastic follow up factor value, q	Stress concentration factor value, K	Purpose
Type 1 Solid Bar SMT	~3.5	1.37	Combined effect of q and K
Type 2 Solid Bar SMT	~2.5	1.7	
pSMT	~4	1.45	Combined effect of q, K and primary pressure load
SBSMT	Controlled with q of 1 to 12	1	Effect of q
SB-pSMT	Controlled with q of 1 to 12	1	Combined effect of q and primary pressure load

Although key featured SMT testing is crucial in verifying the SMT-based design methodology, it is impractical for use in generating data for SMT-based design curves. Wang et al. made significant progress in developing SMT experimental techniques (Wang et al. 2018, 2019, 2020). In particular, the newly developed single-bar SMT (SBSMT) test method and test protocol overcame many challenges associated with SMT key feature experiments and enabled the evaluation of the elastic follow-up effect by using a standard CF specimen without specialized instrumentation and specimen design. In FY 2019, Wang et al. (2019) demonstrated the SBSMT method on Alloy 617, SS316H, and Grade 91 by testing at high temperatures and successfully showed the flexibility of generating SMT-based failure data with a wide range of elastic follow-up values from 1 to 12.

Wang et al. (2020, 2021a, 2021b) extended the SBSMT method to internal pressurized tubular specimens, i.e., SB-pSMT, at 950℃ on Alloy 617. The sustained primary load was introduced by the internal pressure to a tubular SMT sample. The test results from this study along with the original pSMT data on Alloy 617, demonstrated that although internal pressure is within the allowable stress limit per ASME Section III, Division 5, Code Case N-898, the SMT CF cycles to failure were reduced for the cases tested with primary-pressure load. The reduction of SMT CF life because of primary load was found to be dependent on strain ranges and elastic follow-up factors. Approaches to account for the primary-load effect on SMT design curves were discussed in Barua et al. (2020, 2021), and the analysis results show that the EPP strain range analysis procedure naturally captures the primary pressure effect. Barua et al. (2020, 2021) also demonstrated that the EPP-SMT methodology is much simpler to execute than the conventional CF damage analyses through multiple sample problems. The remaining critical factors in finalizing the SMT-based design curves are the methods for extrapolating the design curves to the low strain range region and with longer hold times (such as long hold time of 1,000 h) that are prototypical of plant operations.

2.3 SUMMARY of STANDARD CREEP-FATIGUE AND SMT EXPERIMENTAL DATA ON ALLOY 617

All available standard CF failure data, totaling 105 data points, have been collected, revealing a significant amount of scatter across each condition. The hold times applied in these tests range from a few seconds to a maximum of 4 hours (Wright 2021; Wang et al. 2022). Information regarding the testing temperatures, hold times, strain rates, and sources of the data is summarized in Table 2. The longest hold time data were at 0.01 strain range, with one test at 950 °C, tensile hold time of 2.5-hr and cycles to failure of 386; and two tests at 850 °C with tensile hold time of 4-hr and cycles to failure of 114 cycles and 155 cycles, respectively. The lowest recorded strain ranges are 0.00165 for a 20-second hold time and 0.0018 for a 120-second hold time, both at a temperature of 950 °C (Wang, et al., 2021b). These CF data at temperatures of 800 °C, 850 °C, 950 °C, and 1000 °C have been collected and plotted together in Figure 4. Preliminary analysis indicates that there is no clear relationship between the failure cycles and the testing temperatures and hold times applied during the CF testing, especially at large strain range of 0.01. At lower strain range of 0.003, the lower testing temperature of 800 °C showed slightly longer CF cycles.

Table 2. Summary of the standard creep-fatigue experimental data on Alloy 617.

Standard CF Temperature, ºC	Strain rate, 1/s	Hold time, sec	Strain ranges	Data source
1000	0.001	18 to 1,800	0.01; 0.003	Wright 2021
950	4E-4; 0.001	2 to 9,000	0.01; 0.006; 0.003; 0.00165; 0.0018	Wright 2021 Wang, et al. 2021
850	4E-4; 0.001	60 to 14,400	0.01; 0.006; 0.003;	Wright 2021 Wang et al. 2023
800	0.001	18 to 600	0.01; 0.003	Wright 2021

SMT CF experimental data on Alloy 617 generated in this testing program—including various types of solid bar SMT, pSMT, SBSMT, and SB-pSMT—were primarily collected at 950 °C, with two pSMT data points at 850 °C. This data has been compared with the best-fit pure fatigue curve and the standard CF data at 950 °C, as shown in Figure 5. The elastic follow-up factors for the SMT data ranged from 2 to 12. The CF life cycles are noticeably lower when comparing solid bar SMT to the standard CF data. Additionally, further reductions in CF life are observed when primary pressure load was applied to the SMT experiments, represented in the plot as pSMT. The tensile hold times were 600-seconds for all the pSMT data. The solid bar SMT tests had tensile hold times of 180-seconds to 600-seconds. One of the longest hold time data points for Type 1 SMT, with a 10-hour hold time, was recorded at a nominal strain range of 0.01, resulting in cycles to failure of 150 cycles.

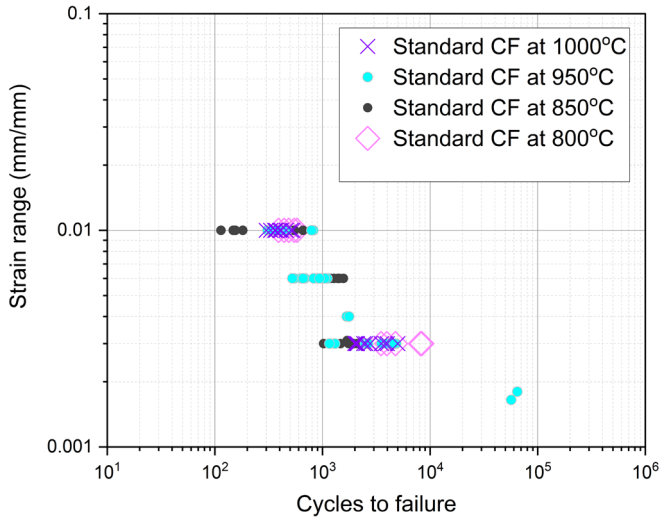

Figure 4. Standard creep-fatigue experimental data on Alloy 617.

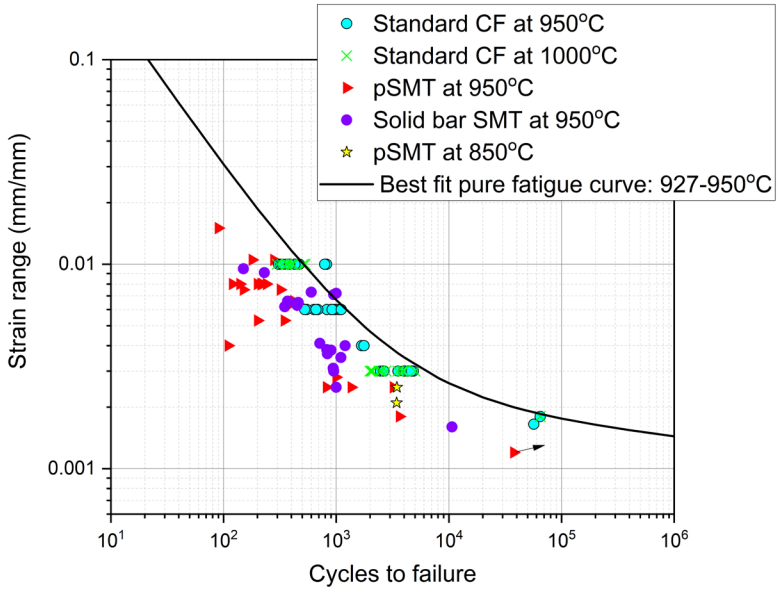

Figure 5. SMT experimental data and standard creep-fatigue data on Alloy 617.

3. EPP-SMT CREEP-FATIGUE DESIGN CURVES FOR ALLOY 617

3.1 DISSIPATED WORK–BASED METHOD FOR CREEP-FATIGUE LIFE PREDICTION

In our recent studies (Hou et al. 2022; Wang et al. 2023), it was concluded that the time fraction-based method was overly conservative, while the dissipated work-based method provided a more accurate prediction of CF performance at elevated temperatures for Alloy 617. The EPP-SMT design fatigue curves are developed based on the dissipated work approach.

In this approach, the dissipated work was calculated from the hysteresis loops, represented by the shaded area in Figure 6.

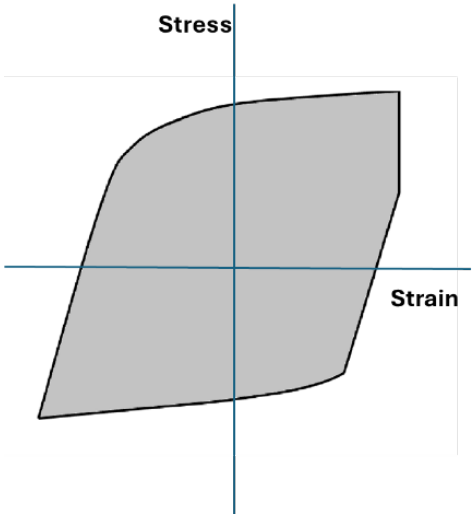

Figure 6. Dissipated work in a hysteresis loop.

There are several key assumptions and developments associated with using the dissipated work-based method for developing the EPP-SMT CF design curves, which are outlined below:

- **Accumulated dissipated work of CF experiments**: The accumulated dissipated work is approximately linearly proportional to the number of applied cycles once the CF process reaches a steady state. This relationship has been demonstrated in our recent studies by analyzing available data alongside the corresponding hysteresis loops (Hou et al. 2023). This finding offers a significant advantage in developing EPP-SMT CF design curve, as it allows for the use of a limited number of CF test cycles to extrapolate results for CF failure cycles effectively.

- **Extrapolation method**: Due to the impractically long test durations required to generate failure data at low strain ranges and extended hold times, a well-calibrated constitutive material model must be developed to accurately describe the material's CF deformation behavior at various temperatures for design curve extrapolation. To this end, ORNL generated data on fatigue and CF deformation behavior across various strain ranges and temperatures to calibrate the material model at ANL (Wang 2024; Hu and Messner 2024). The accumulated dissipated work extrapolated from the newly calibrated material model was compared to the experimental data at temperature range of interest between 850 °C to 954 °C, with the results plotted in Figure 7. The figure shows the two results are comparable, and the material model closely describes the cyclic deformation behavior of the material.

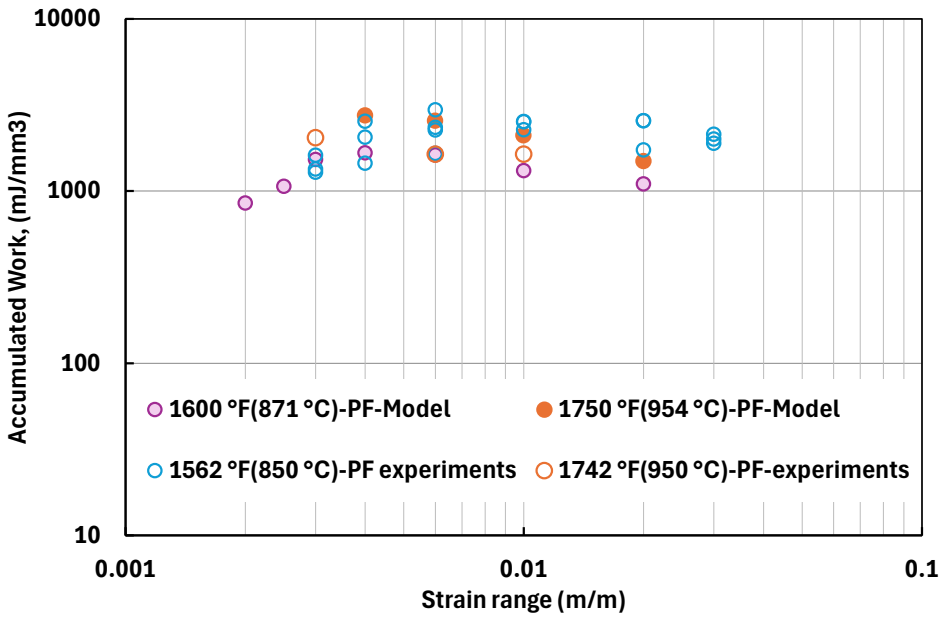

Figure 7. Comparison of the accumulated dissipated work calculated from experiments and that extrapolated from the material model.

- **Failure criteria**: The amount of accumulated dissipated work at failure depends on the testing conditions. However, there is a limited amount of experimental failure data with complete hysteresis loops available from standard CF testing. The CF and pure fatigue data collected in this program were analyzed, and the results are summarized in Figure 8. It shows that pure fatigue generally exhibits higher accumulated dissipated work at failure compared to CF. The accumulated dissipated work at failure for CF tests at 950 °C and 850 °C displayed considerable scatter. The results exhibit showed minimum values of 560 mJ/mm^3 at 950 °C and 506 mJ/mm^3 at 850 °C, and no information is available at lower temperatures. For simplicity, a universal dissipated work value of 500 mJ/mm^3 was used as the cut-off value for predicting CF life cycles from the material model in this study. This assumption presumably leads to a conservative prediction of CF life cycles.

- **Bounding strain range and primary pressure load effect:** In an earlier study by Barua and Messner (2021), it was demonstrated that strain ranges calculated from EPP strain limits analysis on various SMT experiments, with a wide range of elastic follow-up factors from 2 to 4.5, could effectively bound the strain ranges measured experimentally. Furthermore, the impact of primary pressure load on the reduced CF life cycles, as shown in the experimental data (Wang et al. 2017), could be bounded by the increased EPP strain ranges.

- **Elastic follow-up factor in design:** Barua and Messner (2021) compared a theoretical analytical solution using a two-bar model system and concluded that it is reasonable to define cycles to failure by dividing the total cycles from standard CF (with q=1) by the elastic follow-up factor q in a design problem. This scaling method was applied to the solid bar SMT experimental data

generated by Wang et al. (2014 to 2020), and the results demonstrated a reasonable correlation. This approximation allows the use of standard CF data for developing EPP-SMT design curves.

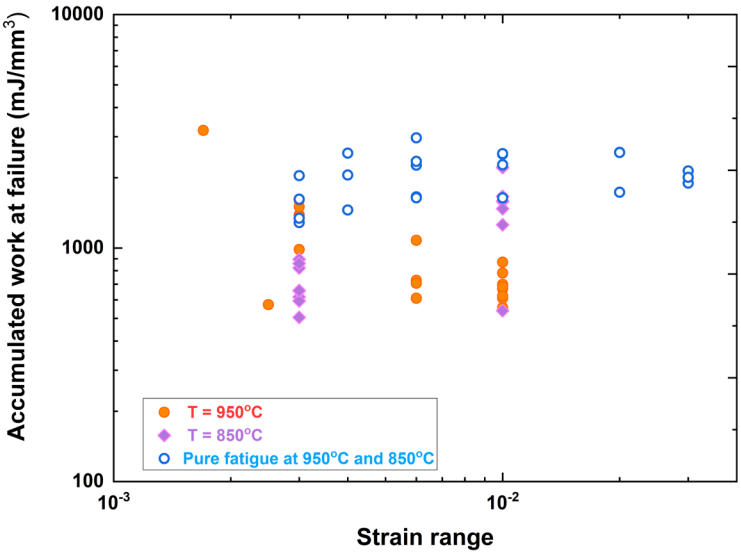

Figure 8. Accumulated dissipated work calculated from standard fatigue and creep-fatigue experimental data on Alloy 617.

3.2 DEVELOPING EPP-SMT CREEP-FATIGUE DESIGN CURVES FOR ALLOY 617

In this study, the cycles to failure were extrapolated using the dissipated work from a limited number of cycles output by the material model at ANL, once it reached steady state. The cut-off value of 500 mJ/mm3 was used as the critical value for CF failure. The analysis considered strain ranges of 0.02, 0.015, 0.012, 0.01, 0.006, 0.004, 0.003, 0.0025, 0.0015, and 0.0013, and hold times of 600-seconds, 1-hr, 10-hr, 100-hr, and 1000-hr at each strain range. The extrapolated CF failure cycles as a function of strain range and hold times were analytically fitted into polynomial curves. These curves represent the 'best-fit' curve for CF cycles to failure.

The EPP-SMT CF design curves are constructed based on the best-fit curves using the conventional approach. Specifically, the design curves are determined as the lower of two curves, obtained by applying a reduction factor of two on the strain range and a reduction factor of twenty on the cycles to failure. This method is illustrated in Figure 9, which develops the EPP-SMT CF design curve with 1-hr hold time at 1750 °F (954 °C).

The available standard CF test data at 950 °C and 1000 °C are plotted in Figure 10 and compared to the EPP-SMT CF curve with a 1-hr tensile hold time at 1750 °F (954 °C) and the associated design curve. It's important to note that most tensile hold times for the test data were relatively short (i.e., less than 1-hr hold time), with only one data point at 4-hr hold. The comparison shows that the proposed EPP-SMT CF curve conservatively envelops all the standard experimental CF data, as all test data results lie to the right of the curve.

Additionally, the pSMT and solid bar SMT experimental data are included in the same plot, which scatter across the CF curve. Even without adjusting for the elastic follow-up factor's effect on the CF cycles, the proposed design curve remains conservative, as demonstrated by the fact that all experimental data points fall to the right of the design curve.

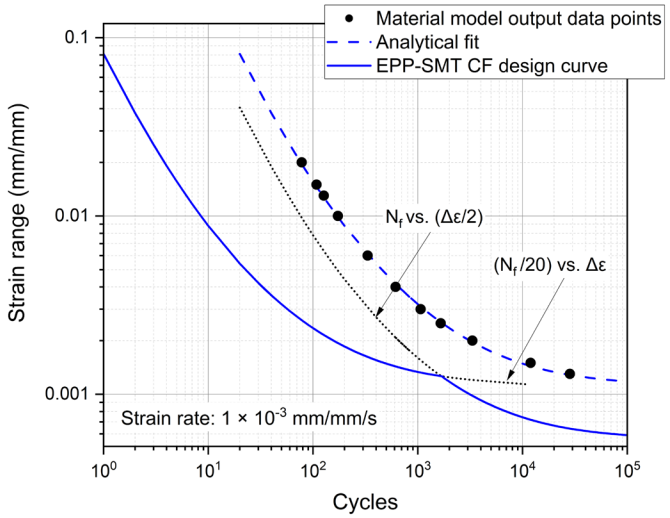

Figure 9. Illustration of the methods for developing EPP-SMT creep-fatigue design curve with a tensile hold time of 1-hr at 1750 °F (954 °C).

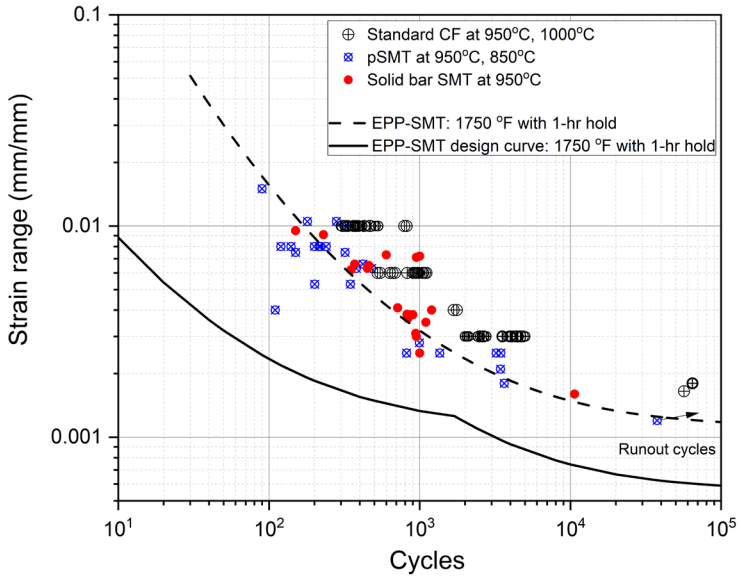

Figure 10. Comparison of the experimental data with the EPP-SMT creep-fatigue curve and design curve with 1-hr hold time at 1750 °F (954 °C).

Further, the ANL material model was used to extrapolate hysteresis loops for standard CF with tensile hold times of 1-hr, 10-hr, 100-hr, and 1000-hr at temperature of 1750 °F (954 °C), 1600 °F (871 °C), 1500 °F (816 °C), 1400 °F (760 °C), 1300 °F (704 °C), and 1200 °F (650 °C). The following key points summarize this part of the study.

- Adding a tensile hold time to a standard CF test at 1300 °F (704 °C) and 1200 °F (650 °C) resulted in a negligible increase in dissipated work, suggesting that stress relaxation behavior at these lower temperatures is minimal.

- No continuous cyclic fatigue curves are available from Alloy 617 Code Case N-898 at 1500 °F (816 °C) and 1400 °F (760 °C). To create a complete set of EPP-SMT CF design curves, the cyclic fatigue curves at these two temperatures were linearly interpolated from the best-fit curves at 1600 °F and 1300 °F. The continuous cyclic fatigue curves at these temperatures were developed using the same approach, i.e., lower of the two curves with a reduction factor of two on the strain range and a reduction factor of twenty on the cycles to failure.

- Plots with the increase in the tensile hold time from 1-hr to 1,000-hr at temperatures above 1300 °F (704 °C) show the changes in the design curves are insignificant, as demonstrated in Figure 11 and Figure 12.

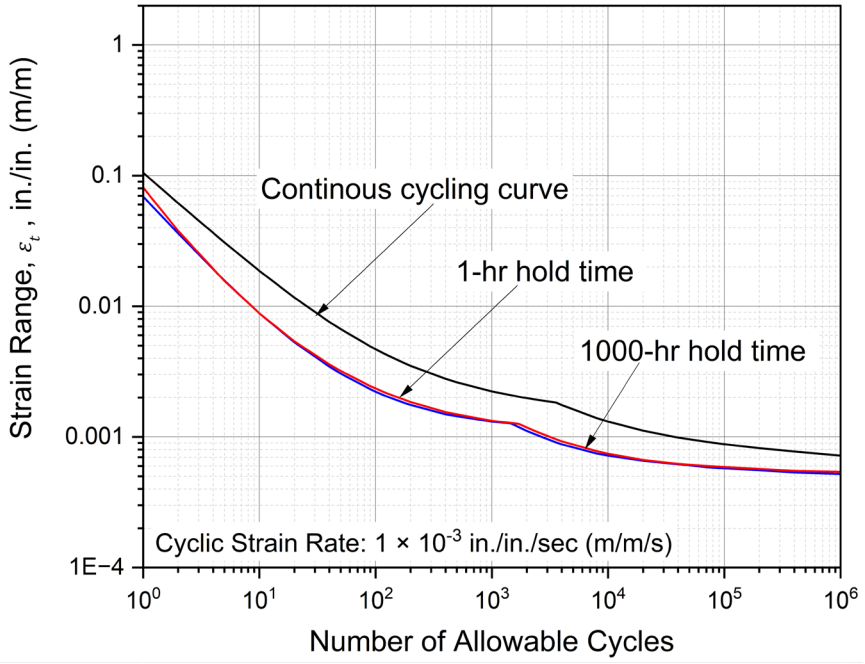

Figure 11. Tensile hold time effect on EPP-SMT creep-fatigue design curves at 1750 °F (954 °C) with an elastic follow-up factor of *q=1*.

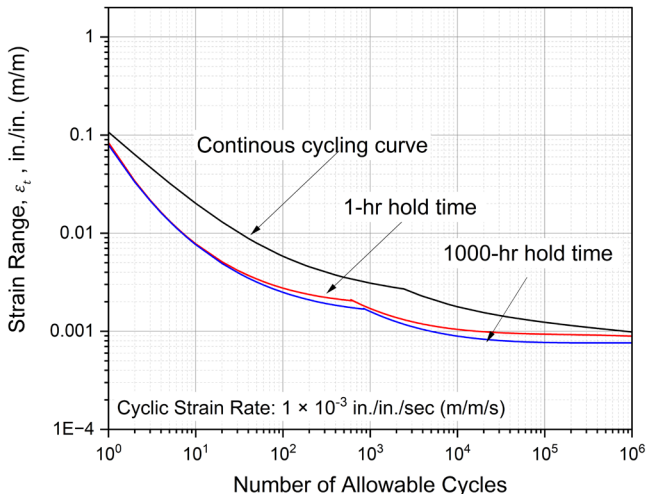

(a)

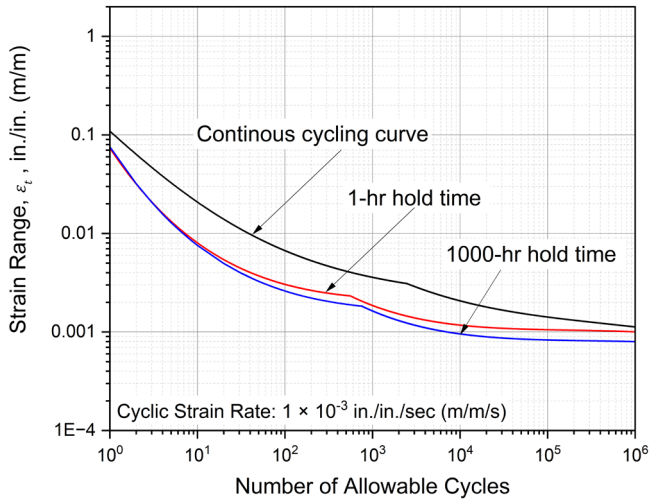

(b)

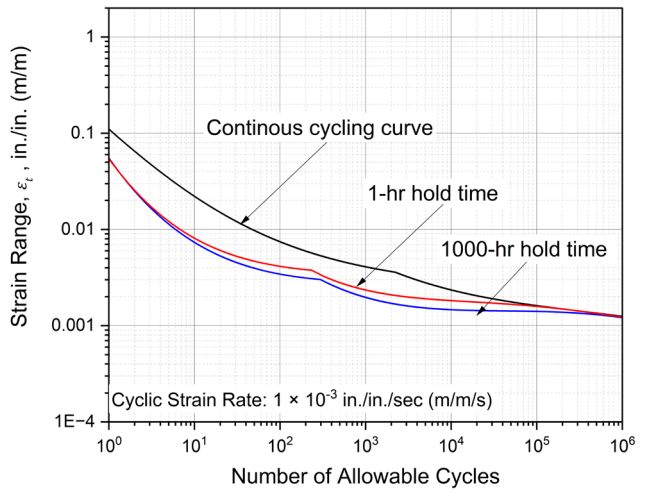

(c)

Figure 12. Tensile hold time effect on EPP-SMT creep-fatigue design curves at temperatures of 1600 °F (a), 1500 °F (b), and 1400 °F (c) with an elastic follow-up factor of *q=1*.

3.3 RECOMMENDED EPP-SMT CREEP-FATIGUE DESIGN CURVES AND TABULATED VALUES FOR ALLOY 617

Based on the analysis and discussions above, it is recommended to adopt following for the CF evaluation using this alternative EPP-SMT approach for Alloy 617:

- Two EPP-SMT CF design curves are provided for each temperature: one for continuous cycling and one that incorporates the maximum hold time effect which is based on a 1,000-hr hold time developed in this study. The EPP-SMT CF design curves for 1750 °F, 1600 °F, 1500 °F, and 1400 °F, with an elastic follow-up factor of q=1, are presented in Figure 13 to Figure 16, and corresponding EPP-SMT CF design strain ranges are summarized in Table 3 to Table 6, in the Appendix A.

- At temperatures of 1300 °F (704 °C) and below, tensile hold time does not significantly impact cyclic life. The continuous cycling curves shall be used for EPP-SMT CF evaluation at temperatures of 1300 °F (704 °C) and below.

- For component design considering the elastic follow-up effect, the allowable cycles should be calculated as the allowable cycles with an elastic follow-up factor of $q = 1$ divided by the maximum elastic follow-up factor found in the EPP analysis of the structure.

4. SUMMARY

This report reviews the EPP-SMT CF evaluation methodology. It summarizes the technical basis for developing the EPP-SMT CF design curves for Alloy 617. The report examines SMT CF experimental data and standard CF testing data on Alloy 617, which serves as the baseline calibration for the EPP-SMT design curves.

To extrapolate the EPP-SMT CF design curves for long hold times, a newly calibrated material constitutive model from ANL was employed to provide the necessary information. A comprehensive set of EPP-SMT CF design curves for Alloy 617 has been developed, accompanied by tabulated design strain range values, all of which are included in this report.

REFERENCE

ASME Boiler and Pressure Vessel Code, (2023), “Rules for construction of Nuclear Facility Components”, Division 1-subsection NB Class 1 Components, American Society of Mechanical Engineers, New York, NY

ASME Boiler and Pressure Vessel Code, (2023), “Rules for construction of Nuclear Facility Components”, Division 5-High Temperature Reactors, American Society of Mechanical Engineers, New York, NY

Barua, B, Messner, M.C., Sham, T.-L., Jetter, R. I., Wang, Y., (2020), "Preliminary description of a new creep-fatigue design method that reduces over conservatism and simplifies the high temperature design process", ANL-ART-194, Argonne National Laboratory, Lemont, IL.

Barua, B, Messner, M.C., Wang, Y., Sham, T.-L., Jetter, R. I. (2021), "Draft Rules for Alloy 617 Creep-Fatigue Design using an EPP+SMT Approach", ANL-ART-227, Argonne National Laboratory, Lemont, IL

Code Case N-898 (2019), “ASME BPVC Code Case for Use of Alloy 617 (UNS N06617) for Class A Elevated Temperature Service Construction, Section III, Division 5”. American Society of Mechanical Engineers, New York, NY

Code Case N-861, “Satisfaction of Strain Limits for Division 5 Class A Components at Elevated Temperature Service Using Elastic-Perfectly Plastic Analysis, ASME Section III Division5”. American Society of Mechanical Engineers, New York, NY

Hou, P, Wang, Y. and Sham, T.-L. (2023a), “A Method for Evaluation of Creep-Fatigue Life at Low Strain Ranges”, Proceedings of the ASME 2023 Pressure Vessels and Piping Conference, PVP2023-106512, American Society of Mechanical Engineers, Atlanta, Georgia.

Hou, P, Wang, Y. and Sham, T.-L. (2023b), “Notch Effect On Creep-Fatigue Behavior Of Alloy 617 At Elevated Temperature” Proceedings of the ASME 2023 Pressure Vessels and Piping Conference, PVP2023-106503, American Society of Mechanical Engineers, Atlanta, Georgia.

T. Hu and M.C. Messner (2024), “Simplified inelastic constitutive models for ASME Section III, Division 5 design by inelastic analysis”, ANL-ART-284, Argonne National Laboratory, Lemont, IL.

Jetter, R. I., (1998), “An Alternate Approach to Evaluation of Creep-Fatigue Damage for High Temperature Structural Design Criteria,” PVP-Vol. 5 Fatigue, Fracture and High Temperature Design Methods in Pressure Vessel and Piping, Book No. H01146 – 1998, American Society of Mechanical Engineers Press, New York, New York.

Kasahara, N., Nagata, T., Iwata, K. and Negishi, H., (1995), “Advanced Creep-Fatigue Evaluation Rule for Fast Breeder Reactor Components: Generalization of Elastic Follow-up Model,” Nuclear Engineering and Design, Vol. 155, pp. 499-518.

Takahura, K., Ueta, M., Dousaki, K. Wada, H., Hayashi, M., Ozaki, H., and Ooka, Y., (1995), "Elevated Temperature Structural Design Guide for DFBR in Japan," Transactions of the 13th International Conference on Structural Mechanics in Reactor Technology, Vol. 1, P380.

Messner, M. C., Sham, T. L., Wang, Y., and R. I. Jetter, R.I. (2018), “Evaluation of methods to determine strain ranges for use in SMT design curves”, ANL-ART-138, Argonne National Laboratory, Lemont, IL.

Messner, M.C. (2022). ASME Code Revisions to Incorporate 316H and Alloy 617 Viscoplastic Constitutive Models to Section III, Division 5 and Code Case N-898 (No. ANL-ART-249). Argonne National Lab.(ANL), Argonne, IL (United States).

Messner, M.C. and Sham, T.L. (2021). A Viscoplastic Model for Alloy 617 for Use with the ASME Section III, Division 5 Design by Inelastic Analysis Rules. In Pressure Vessels and Piping Conference (Vol. 85314, p. V001T01A034). American Society of Mechanical Engineers.

Messner, M. C., Jetter. B, and Sham, T. L. (2019), "A Method for Directly Assessing Elastic Follow Up in 3D Finite Element Calculations," Proceedings of the ASME 2019 Pressure Vessels & Piping Conference, PVP2019-93644, American Society of Mechanical Engineers, New York.

Wang, Y., Jetter, R. I., Krishnan, K., and Sham, T.-L (2013) "Progress Report on Creep-Fatigue Design Method Development Based on SMT Approach for Alloy 617", ORNL/TM-2013/349, Oak Ridge National Laboratory, Oak Ridge, TN.

Wang, Y., Jetter, R. I. and Sham, T.-L (2014), "Application of Combined Sustained and Cyclic Loading Test Results to Alloy 617 Elevated Temperature Design Criteria", ORNL/TM-2014/294, Oak Ridge National Laboratory, Oak Ridge, TN.

Wang, Y., Jetter, R. I., Baird, S. T., Pu, C. and Sham, T.-L. (2015), "Report on FY15 Two-Bar Thermal Ratcheting Test Results", ORNL/TM-2015/284, Oak Ridge National Laboratory, Oak Ridge, TN.

Wang, Y., Jetter, R. I., and Sham, T.-L. (2016a), "FY16 Progress Report on Test Results In Support Of Integrated EPP and SMT Design Methods Development" ORNL/TM-2016/330, Oak Ridge National Laboratory, Oak Ridge, TN.

Wang, Y., Jetter, R. I., and Sham, T.-L. (2016b), "Preliminary Test Results in Support of Integrated EPP and SMT Design Methods Development", ORNL/TM-2016/76, Oak Ridge National Laboratory, Oak Ridge, TN.

Wang, Y., Jetter, R.I., and Sham, T.-L. (2017a), "Report on FY17 Testing in Support of Integrated EPP-SMT Design Methods Development", ORNL/TM-2017/351, Oak Ridge National Laboratory, Oak Ridge, TN.

Wang, Y., Jetter, and Sham, T.-L. (2017b), "Pressurized Creep-Fatigue Testing of Alloy 617 Using Simplified Model Test Method", Proceedings of the ASME 2017 Pressure Vessels and Piping Conference, PVP2017-65457, American Society of Mechanical Engineers, New York, NY.

Wang, Y., Jetter, R. I., Messner, M., Mohanty, S., and Sham, T.-L. (2017c), "Combined Load and Displacement Controlled Testing to Support Development of Simplified Component Design Rules for Elevated Temperature Service", Proceedings of the ASME 2017 Pressure Vessels and Piping Conference, PVP2017-65455, American Society of Mechanical Engineers, New York, NY.

Wang, Y., Jetter, R. I., Messner, M., and Sham, T.-L. (2018), "Report on FY18 Testing Results in Support of Integrated EPP-SMT Design Methods Development", ORNL/TM-2018/887, Oak Ridge National Laboratory, Oak Ridge, TN.

Wang, Y., Jetter, R. I., Messner, M., and Sham, T.-L. (2019), "Development of Simplified Model Test Method for Creep-fatigue Evaluation", Proceedings of the ASME 2019 Pressure Vessels and Piping Conference, PVP2019-93648, American Society of Mechanical Engineers, New York, NY.

Wang, Y., Hou, P., Jetter, R. I., and Sham, T.-L. (2020), "Report on FY2020 Test Results in Support of the Development of EPP Plus SMT Design Method", ORNL/TM-2020/1620, Oak Ridge National Laboratory, Oak Ridge, TN.

Wang, Y., Hou, P., Jetter, R. I., and Sham, T.-L. (2021a), "Evaluation of the Primary-Load Effects on Creep-Fatigue Life of Alloy 617 Using Simplified Model Test Method", Proceedings of the ASME 2021 Pressure Vessels and Piping Conference, PVP2021-61658, American Society of Mechanical Engineers, New York, NY

Wang, Y., Hou, P., Jetter, R. I., and Sham, T.-L. (2021b), "Report on FY2021 Test Results in Support of the Development of EPP Plus SMT Design Method", ORNL/TM-2021/2159, Oak Ridge National Laboratory, Oak Ridge, TN.

Wang, Y. Jetter, R. I., and Sham, T.-L. (2023), "Experimental and analytical verification of ASME Section III, Division 5 creep-fatigue design rules", Proceedings of the ASME 2017 Pressure Vessels and Piping Conference, PVP2024-123351, American Society of Mechanical Engineers, New York, NY.

Wright, R. N. (2021). "Draft ASME Boiler and Pressure Vessel Code Cases and Technical Bases for Use of Alloy 617 for Construction of Nuclear Components Under Section Ill, Division 5". INL/EXT-15-36305, Idaho National Laboratory, Idaho Falls, Idaho.

APPENDIX.
EPP-SMT CREEP-FATIGUE DESIGN CURVES FOR ALLOY 617 WITH ELASTIC FOLLOW UP FACTOR OF *q=1*

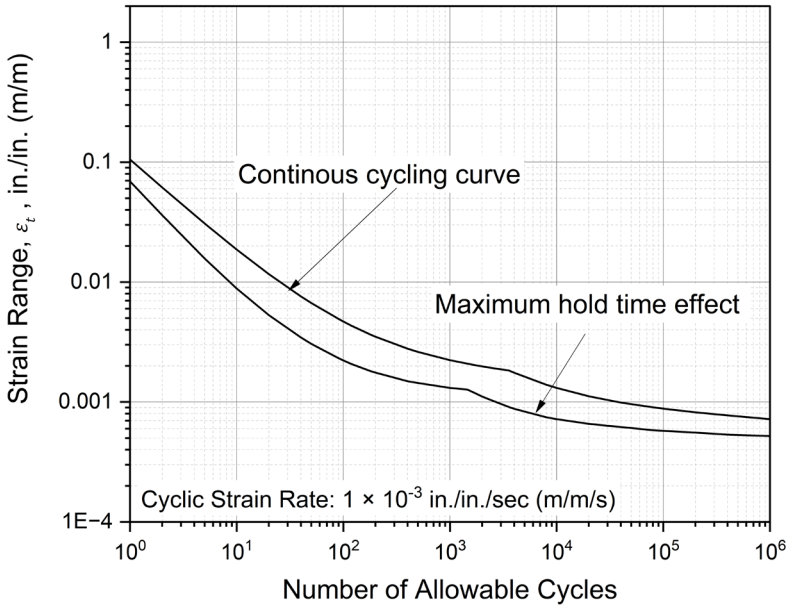

.

Figure 13. EPP-SMT creep-fatigue design curves at 1750 °F with an elastic follow-up factor of q=1.

Table 3. EPP-SMT creep-fatigue design strain range for Alloy 617 at 1750 °F (954 °C) with an elastic follow-up factor of *q=1*.

Allowable cycles	Continuous cycling	With maximum hold time effect
10	0.01868	0.008830
20	0.01166	0.005300
40	0.0076	0.003450
100	0.00469	0.002220
200	0.0035	0.001760
400	0.00279	0.001490
1000	0.00223	0.001310
2000	0.00198	0.001110
4000	0.00175	0.000878
10000	0.00131	0.000718
20000	0.00112	0.000657
40000	0.00099	0.000618
1.00E+05	0.00088	0.000575
2.00E+05	0.00082	0.000555
4.00E+05	0.00077	0.000535
1.00E+06	0.00072	0.000520

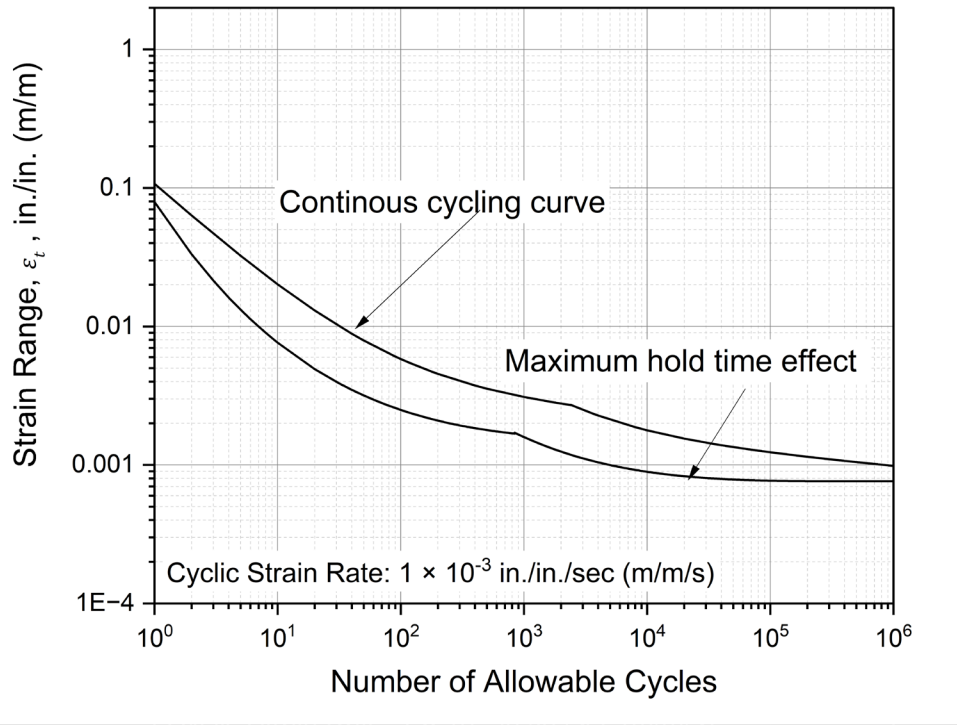

Figure 14. EPP-SMT creep-fatigue design curves at 1600 °F with an elastic follow-up factor of *q=1*.

Table 4. EPP-SMT creep-fatigue design strain range for Alloy 617 at 1600 °F (871 °C) with an elastic follow-up factor of *q=1*.

Allowable cycles	Continuous cycling	With maximum hold time effect
10	0.02015	0.007630
20	0.01303	0.004920
40	0.00885	0.003490
100	0.00582	0.002500
200	0.00455	0.002090
400	0.00375	0.001840
1000	0.00310	0.001590
2000	0.00278	0.001250
4000	0.00227	0.001050
10000	0.00178	0.000893
20000	0.00155	0.000829
40000	0.00139	0.000792
1.00E+05	0.00124	0.000770
2.00E+05	0.00115	0.000764
4.00E+05	0.00107	0.000762
1.00E+06	0.00098	0.000762

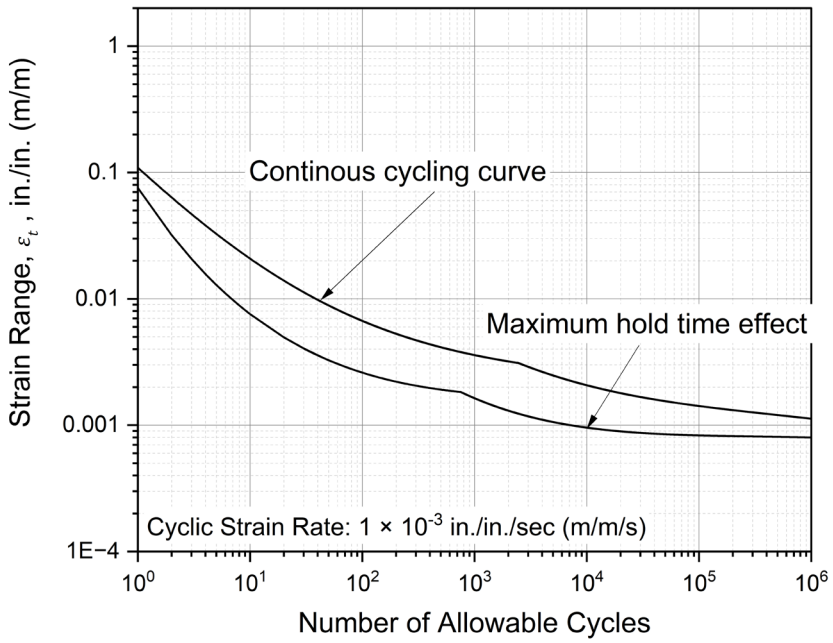

Figure 15. EPP-SMT creep-fatigue design curves at 1500 °F with an elastic follow-up factor of *q=1*.

Table 5. EPP-SMT creep-fatigue design strain range for Alloy 617 at 1500 °F (816 °C) with an elastic follow-up factor of *q=1*.

Allowable cycles	Continuous cycling	With maximum hold time effect
10	0.020827	0.007568
20	0.01394	0.004958
40	0.009825	0.003570
100	0.006691	0.002607
200	0.005291	0.002210
400	0.004368	0.001968
1000	0.003587	0.001634
2000	0.003197	0.001303
4000	0.002645	0.001105
10000	0.00207	0.000956
20000	0.001793	0.000893
40000	0.001599	0.000856
1.00E+05	0.001418	0.000830
2.00E+05	0.001316	0.000820
4.00E+05	0.001229	0.000811
1.00E+06	0.001125	0.000799

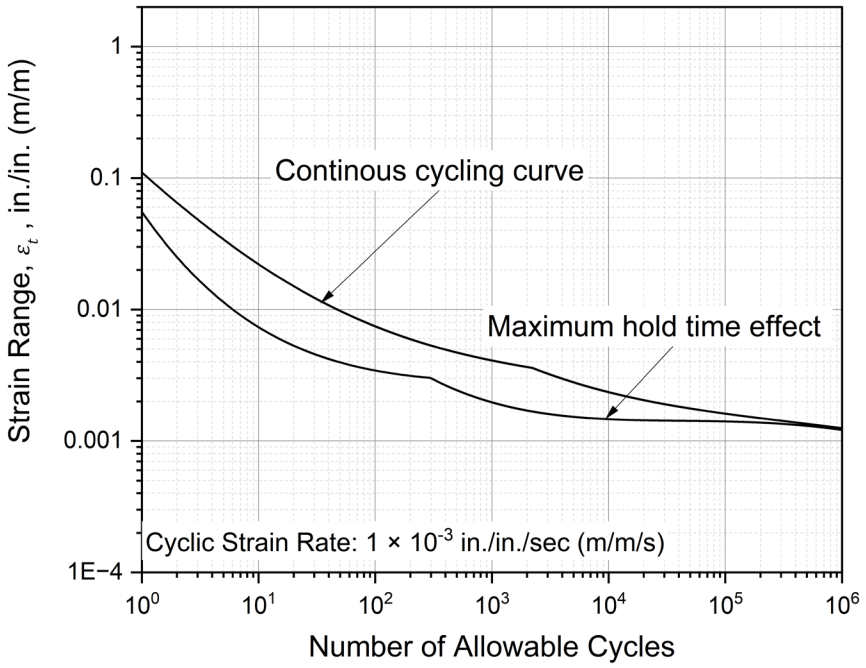

Figure 16. EPP-SMT creep-fatigue design curves at 1400 °F with an elastic follow-up factor of *q=1*.

Table 6. EPP-SMT creep-fatigue design strain range for Alloy 617 at 1400 °F (760 °C) with an elastic follow-up factor of *q=1*.

Allowable cycles	Continuous cycling	With maximum hold time effect
10	0.022127	0.007368
20	0.015048	0.005304
40	0.010764	0.004182
100	0.007456	0.003412
200	0.005956	0.003117
400	0.007524	0.002652
1000	0.004884	0.001969
2000	0.003728	0.001706
4000	0.002978	0.001559
10000	0.002353	0.001465
20000	0.002046	0.001437
40000	0.001826	0.001425
1.00E+05	0.001615	0.001408
2.00E+05	0.001491	0.001379
4.00E+05	0.001383	0.001326
1.00E+06	0.00125	0.001213